Confined kerosene vapor explosion: Severity prediction laws based on numerical simulations

Nicolas Gascoin, Philippe Gillard

Energy Fuels **2010,** *24,* 404–418 · DOI:10.1021/ef900909e
Published on Web 10/07/2009

energy&fuels
article

Confined Kerosene Vapor Explosion: Severity Prediction Laws Based on Numerical Simulations.

N. Gascoin* and P. Gillard

PRISME Institute 63, avenue de Lattre de Tassigny, 18020 Bourges Cedex, France

Received August 20, 2009. Revised Manuscript Received September 24, 2009

The vulnerability of aircraft, if attacked by conventional weapons, depends notably on the possibility to initiate and to propagate a combustion reaction in the multicompartmented kerosene tanks. After a review of the related mechanisms and existing studies, the numerical simulation tool MIRAGE (french acronym for gas flow adaptable and transient reactive modeling) is used extensively to investigate the effects of four parameters: the ignition energy (from 5 to 1000 J), the equivalence ratio in air (from 0.3 to 2.19), the tank pressure (from 1 to 1.8 bar absolute), and its volume (from 0.4 to 2 m^3). A detailed kinetic mechanism is considered (207 species, 1592 reactions) to properly represent the chemistry. The maximum pressure after explosion is found to depend mainly on the initial pressure and on the equivalence ratio, but not on the tank volume or the applied energy. A critical value of the energy, corresponding to the limit between ignition and no ignition, is shown depending on the equivalence ratio but also on the initial pressure of the tank. Thanks to these results of "numerical experiments", empirical laws are proposed to estimate the overpressure and its dynamic depending on the preceding four parameters. These laws are also applied to some test cases of the literature, with good agreement.

1. Introduction

To conduct vulnerability studies on air systems (aircraft, UAV, helicopter), the french military agency DGA (Délégation Générale à l'Armement) is developing a modular software called PLEIADES/A, with a related module ALBAS dedicated to scenarios involving conventional and antiaircraft weapons.[1] In this framework, it is required to estimate how ammunition that is impacting an aircraft can cause its destruction.

The kerosene tanks are composed of several interconnected compartments, which are pressurized with outlet air at about 0.8 barg (gauge bar) over the ambient pressure. Due to the evaporation of the liquid kerosene, a gaseous reactive phase appears. If a sufficient amount of energy is provided to this gas phase, a combustion reaction can be initiated. This turns into an explosion due to the confinement in the tank. Several factors impact this explosion. The quantity of kerosene in gas phase, which is linked to the saturation vapor pressure, depends on the ambient temperature and pressure. This acts on the equivalence ratio, which controls in relation to the ignition energy the possibility to observe an explosion, whose severity varies with the tank volume. The influence of the multicompartments configuration is not studied in this paper because it is preferred to first focus on the ignition and propagation of the flame in one volume before extending to several compartments with possible pressure-controlled venting systems.

In the continuity of previous work,[2,3] it is chosen to investigate the kerosene explosion in gas phase because the combustion initiation first appears in the gaseous reactive fluid. This assumption has been validated by comparing the data from the open literature. Several experimental studies exist on combustion of kerosene vapor induced by liquid evaporation.[3,4] The gaseous explosions of light hydrocarbons from methane to propane generally present explosion pressure on the initial ratio of 6−9 depending on the conditions and fuel nature.[5−8] When considering a liquid phase in the tank, this ratio decreases slightly, for example from 7.18 to 7.1 with a liquid loading of 200 $kg \cdot m^{-3}$.[4] This diminishing trend is known and it is attributed to the heat sink that the liquid represents. The main difference between the combustion of gas and of fuel vapors is the equivalence ratio, which cannot vary independently from the temperature and pressure conditions for the latest.

The way the energy is provided to the reactive system is complex because it requires numerous data on the aircraft attack and it is difficult to generalize. Indeed, when the ammunition impacts the metallic surface of the tank, it looses some energy. This can be computed by the Thor law.[1,3] But it is not possible to evaluate the number, the size, and the energy of the possible produced fragments, which may participate to a time-delayed multipoint ignition. Furthermore, the

*Corresponding author. Telephone: +33.248.238.473. Fax: +33.248.238.871. E-mail: Nicolas.Gascoin@bourges.univ-orleans.fr.

(1) Puech R., Domingues-Vinhas J. L. ALBAS: an integrated software for carrying out parametric vulnerability/lethality PLEIADES/A calculations. *NATO RTO Specialist's Meeting AVT-153 on Weapon/Target Interaction Tools for use in Tri-Service Applications*: Canada, 13−15 October 2008.
(2) Sochet, I.; Gillard, P. *J. Loss Prev. Process Ind.* **2002**, *15*, 335–345.
(3) Sochet I., Pascaud J.-M., Gillard P. *J. Phys. IV* (*France*) **2002**, *12*, DOI: 10 1051/Jp4 20020312.
(4) Shepherd J. E., Krok J. C., Lee J. J. Spark Ignition Energy Measurements in Jet A, *Explosion Dynamics Laboratory Report FM97−9*; Graduate Aeronautical Laboratories, California Institute of Technology: May 3, 1999, Revised January 24, 2000.
(5) Razus, D.; Movileanu, C.; Brinzea, V.; Oancea, D. *Fuel* **2007**, *86*, 1865–1872.
(6) Ogle, R. A., *Process Saf. Prog.* **1999** *18*, No.3.
(7) Molkov, V.; Dobashi, R.; Suzuki, M.; Hirano, T. *J. Loss Prev. Process Ind.* **2000**, *13*, 397–409.
(8) Kunz, O. *Combustion Characteristics of Hydrogen- and Hydrocarbon-Air Mixtures in Closed Vessels*. Thesis, University of Stuttgart, Aerospace Department: Germany, 1998.

ammunition speed is highly supersonic. A shock in front of the projectile may appear and the resulting energy transfer is not trivial. For example at Mach 2, the Hugoniot-Rankine tables of shock waves give a temperature ratio of about 0.56 and a pressure ratio of 0.13. Thus the local conditions of initiation could be largely different from the overall tank conditions. For flight altitude between 0 and 10 000 m, the absolute pressure (in absolute bar, bara) of the gaseous phase ranges from 1 to 1.8 bara and the temperature from 218 to 338 K. Furthermore, if the projectile first impacts the liquid phase before traversing the gas, a spray can be generated. The spray generation is a very challenging task if the conditions of impact (angle, velocity, speed) are not well-defined.

1.1. Vapor and Gas Explosions. The phenomena involved in gas explosions have been extensively studied.[7,9−12] The maximum pressure reached after explosion is proportional to the initial one.[5,13] Several other parameters can impact on this proportionality: the nature of the fuel,[4,6,7] the fuel concentration[14,15] (nonlinear effect), the heterogeneity of species concentration,[9] the presence of other compounds,[5,16] the temperature,[17] the turbulence,[13] the position of the ignition point[14] and its distance in regards with the possible venting system,[18] the opening pressure of venting system,[9] and the vent area[19] Despite the lower and upper flammable limits, some works report an inflammation outside these values. This is due to their dependence on the temperature and pressure conditions.[6,20,21]

The velocity of pressure rise depends on the tank volume but also on the distance between the ignition point and the discharge hole if applicable.[15,22] When this distance increases, the flame speed rises because of the turbulence development.[9,11,23] The presence of obstacles acts in the same way for the same reason.[14] Considering two or more interconnected volumes, due to the compression of fresh gases, the maximum pressure after explosion is the highest in the volume, which is the farthest from the ignition point.[24] This phenomenon is called pressure pilling or precompression effect. Furthermore, if the volumes do not have the same size, some pressure oscillations can appear due to different dynamic of pressure rises.[22] The flame propagates more easily from a big volume to a small one than from a small one to a big one. But the time of transmission between them depends on the initial pressure.[19]

Numerous studies also focus on the severity of explosions, which is often linked to the initial fuel concentration[6,21] or to a venting system.[9,12] Several laws are proposed in order to set the dimension of the vent,[12] to estimate the flame speed,[10,16,25] or the external pressure wave.[7,26] Nevertheless, no laws exist to predict the dynamic load on mechanical structure in order to give its dimension to ensure its strength.

1.2. Explosion Severity. The K_G (for gas explosion) or K_{st} (for dust explosion), the pressure rise coefficient, is the maximum value of the time derivative of pressure multiplied by the cubic root of the volume. In this study, the notation "K_G" will be used because it is related to the gas explosions. It can be found under the name of explosion index or severity factor. It represents the severity of the explosion and it allows reproducing an explosion at small laboratory scale. Thus, the severity of largest explosions can be deduced from these experiments thanks to this explosion index, the K_G. It is one of the most common parameter in the field of safety and hazard.[8,20] For the software ALBAS, it will be a key parameter to estimate the dynamic load on the tank structure to estimate its mechanical strength. The estimation of the K_G depending on the configuration (geometry, fuel nature, conditions of temperature and pressure) is often obtained experimentally, and only few studies try to propose an empirical law.[8,27,28] Notably, Dahoe et al. propose a simple—but very interesting—formulation by considering the flame thickness in dust explosion.[27] This requires knowing the maximum explosion pressure and the flame speed. But this approach is mainly developed for dust explosion because the large flame thickness impacts drastically on the general cube-root law, which is commonly used to determine the K_{st}. Another law, proposed by Van den Bulck,[28] is dedicated to gaseous explosions. It uses a linear approach between the conversion rate of the fuel and the pressure. This approximation may be related to the law used in combustion of solid monopropellants. But for gases, the temperature has a great impact on the kinetics, more than the pressure. The thermodynamic equilibrium approach, which is used by Van den Bulck, is also convenient. But with this assumption, the detailed chemistry of the two-steps combustion model is not considered for the hydrocarbon fuel (pyrolysis of the fuel then followed by the combustion of the byproduct). Nevertheless, his formulation appears to be interesting and give a good agreement with the validation data.

Based on these experimental studies, some authors propose different laws to estimate the severity of explosions. Most of them are relative to vented explosions,[8,25,29−33] with or without obstacles considerations. They are mainly based on isentropic relationships and intrinsic parameters of the

(9) Bjerketvedt, D.; Bakke, J. R.; van Wingerden, K. *J. Hazard. Mater*. **1997**, *52*, 1–150.
(10) Cleaver, R. P.; Robinson, C. G. *J. Hazard. Mater*. **1996**, *45*, 27–44.
(11) Dobashi, R. *J. Loss Prev. Process Ind*., **1997**, Vol. *10*. No. 2, pp 83−89.
(12) Tamanini, F.; Chaffee, J. L. *Process Saf. Prog*. **2000**, *19*, No. 4.
(13) Amyotte, P. R.; Patil, S.; Pegg, M. J. *Inst. Chem, Eng., Trans IChemE* **2002**, Vol *80*, Part B.
(14) Kindracki, J.; Kobiera, A.; Rarata, G.; Wolanski, P. *J. Loss Prev. Process Ind*. **2007**, *20*, 551–561.
(15) Larsen, O.; Eckhoff, R. K. *J. Loss Prev. Process Ind*. **2000**, *13*, 341–347.
(16) Miao, H; Huang, Q; Hu, E; Huang, Z; Jiang, D *Energy Fuels* **2009**, *23*, 1431–1436.
(17) Tang, C.; Huang, Z.; Jin, C.; He, J.; Wang, J.; Wang, X.; Miao, H. *Int. J. Hydrogen Energy* **2009**, *34*, 554–561.
(18) Kumar, R. K. Vented Combustion of Hydrogen-Air Mixtures in a Large Rectangular Volume. 44th AIAA Aerospace Sciences Meeting and Exhibit, Reno, Nevada, January 9−12, 2006.
(19) Razus, D.; Oancea, D.; Chirila, F.; Ionescu, N. I. *Fire Safety J*. **2003**, *38*, 147–163.
(20) Schröder, V.; Holtappels, K. Explosion Characteristics of Hydrogen-Air and Hydrogen-Oxygen Mixtures at elevated Pressures. International Conference on hydrogen safety, Congress Palace, Pisa, Italy, September 8−10 2005.
(21) Jo, Y.-D.; Park, K.-S. *Process Saf. Prog*. **2004**, *23*, No. 4.
(22) Hashimoto, A.; Matsuo, A. *J. Loss Prev. Process Ind*. **2007**, *20*, 455–461.
(23) Alexiou, A.; Andrews, G. E.; Phylaktou, H. *J. Loss Prev. Process Ind*. **1996**, *9*. No. 5, pp 351−356.
(24) Rogstadkjernet, L. *Combustion of Gas in Closed, Interconnected Vessels: Pressure Piling*; Thesis, Department of Physics and Technology, University of Bergen: Norway, 2004.
(25) Razus, D. M.; Krause, U. *Fire Saf. J*. **2001**, *36*, 1–23.
(26) Forcier, T.; Zalosh, R. *J. Loss Prev. Process Ind*. **2000**, *13*, 411–417.
(27) Dahoe, A.; Zevenbergen, J.; Lemkowicz, S.; Scarlett, B. *J. Loss Prev. Process Ind*. **1996**, *9*, 33–44.
(28) Van den Bulck, E. *J. Loss Prev. Process Ind*. **2005**, *18*, 35–42.
(29) Park, D. J.; Lee, Y. S.; Green, A. R. *J. Hazard. Mater*. **2008**, *155*, 183–192.
(30) Park, D. J.; Lee, Y. S. *Kor. J. Chem. Eng*. **2009**, *26* (2), 313–323.
(31) Molkov, V. V. *J. Loss Prev. Process Ind*. **2001**, *14*, 567–574.
(32) Russo, P.; Di Benedetto, A. *Trans IChemE, B* **2007**, DOI: 10.1205/psep.04268.
(33) Di Benedetto, A.; Salzano, E.; Russo, G. *Fire Saf. J*. **2005**, *40*, 282–298.

flame and the fuel nature, but unfortunately they use several arbitrary coefficients which limit their range of validity. Some studies also report empirical laws, which tend to estimate the minimum ignition energy required to initiate a combustion reaction.[4,8] These are exactly opposite to the present work because the energy is known here and the overpressure due to the explosion is of interest.

Some methods have been developed to generalize the explosion data to find a way of predicting the blast load on structures. Unfortunately, these approaches correspond to unconfined explosions. The most common are the TNO multienergy[34] and the TNT[35] methods. The TNO model considers a hemispheric gaseous reactive phase, and it is based on a coefficient ranging from 1 (weak deflagration) to 10 (strong detonation) that should be previously given. This is the major drawback, even if tables are available to estimate it. The TNT method converts the available energy in the gaseous phase into a weight equivalent of TNT. This method is not the most suitable for considering the vapor cloud explosion.[36] There are other methods which exist, and they are often based on CFD approach, which is simplified by a 1D spherical approach.[36]

The numerical simulation is a very efficient way to manage such vulnerability studies because the experiments are difficult to conduct. Thus, the computations realized in this study are used to propose empirical laws for the prediction of the K_G and of the explosion pressure for kerosene vapor.

1.3. Kinetic Modeling of Kerosene Combustion. Several denominations exist to qualify the aeronautical fuels. The unification norm (AFQ RJOS which stands for aviation fuel quality: requirements for jointly operated systems) regroups the American norm (ASTM D1655−04a) and the English one (Def Stan 91).[37] The "joint fuelling system check list" allows to verify whether a fuel corresponds to this norm or not. The military American kerosenes are often noted JP, for jet propellant, from 1 to 10 depending on their specificity (freezing point, flash point, etc.). The commercial grades are Jet-A or Jet-A1 for example.[38] The Jet-A1 is similar to the JP-8 (called F-35 by NATO) with a flash point of 311 K and a melting point of 226 K. It presents a combustion enthalpy around 42.8 $MJ \cdot kg^{-1}$ and a density of 775−840 $kg \cdot m^{-3}$ at 288 K. The main differences consist in addition of some antifreezing and anticorrosion additives.

The mean molecular formula of kerosene is often considered to be $C_{11}H_{21}$ (mean value between alkenes and alkanes[39]), but this depends on its production origin. Numerous detailed combustion mechanisms exist[40−45] and several surrogates are considered to be representative of the kerosene.[46] Dagaut and Cathonnet[45] consider a mixture of 74 vol % of decane, 11 vol % of n-propylcyclohexane, and 15 vol % of n-propylbenzene, whereas the US Air Force suggest to consider 12 compounds with only 16.08 wt % of decane and 22.54 wt % of dodecane, the major compound. If the majority of kinetic mechanisms gives a very good overall representation of the kerosene combustion,[45] in details, some fail to describe precisely the formation or consumption of byproduct.

2. Preliminary work

Before conducting the parametric work (Section 3), the choices of the kerosene surrogate and of the numerical tool have been notably justified in the present section.

2.1. Choice of the Kerosene Surrogate. The kerosene is often studied with simplified models or surrogates because of its complex composition with more than one hundred species. A test has been conducted to observe the difference that can be obtained with several fuel compositions. For the decane and the mixture—proposed by Dagaut and Cathonnet[45]—(Figure 1a), the discrepancy observed on the temperature after combustion depends on the initial temperature of the reactive mixture. It varies from 10 K (for a mixture at an initial temperature of 850 K) to 4 K (for a mixture at 2000 K). A corresponding pressure differential, from 21 to 4 mbar, is observed between the same cases (Figure 1b). The difference also appears to be negligible on the ignition delay, but it is more noticeable on the maximum rate of pressure rise (Table 1). This very high dynamic pressure parameter is due to the numerical integration time step and it is not physical. The decane can be reasonably chosen as the kerosene surrogate in this study because it presents the advantage to be a pure component. Thus, it could be more feasible to compare the results with open literature data or with experimental ones. The mechanism of Dagaut and Cathonnet[45] is used in all the present work.

2.2. Range of Study. The gaseous kerosene content depends on the liquid phase evaporation, thus on the pressure and temperature conditions. The vaporization temperature $T_{vap}(P)$ at a given pressure P or the saturation pressure $P_{sat}(T)$ at a fixed temperature T can be computed by the following equations.

$$T_{vap}(P) = \frac{T_{vap}(P_{atm}) \times T_C \times \ln(P_C)}{T_C \times \ln(P_C) + (T_{vap}(P_{atm}) - T_C) \times \ln(P)} \quad (1)$$

$$P_{sat}(T) = P_C \times \exp\left(1 - \frac{T_{vap}(P_{atm})}{T} \times \frac{T_C}{T_C - T_C(P_{atm})}\right) \quad (2)$$

(34) van den Berg, A. C.; Versloot, N. H. A. *J. Loss Prev. Process Ind.* **2003**, *16*, 111–120.
(35) Pierorazio, A. J.; Thomas, J. K.; Kolbe, M.; Goodrich, M. L. *Internal Explosion Methodologies*; Proceedings of Canadian Society for Chemical Engineering (CSChE), Sherbrooke, October 18, 2006
(36) Beccantini, A.; Malczynski, A.; Studer, E. *Comparison Of TNT-Equivalence Approach, TNO Multi-Energy Approach and a CFD Approach In Investigating Hemispheric Hydrogen-Air Vapor Cloud Explosions*; Proceedings of the 5th International Seminar on Fire and Explosion Hazards, Edinburgh, UK, April 23−27, 2007.
(37) Joint Inspection Group. *Aviation Fuel Quality Requirements For Jointly Operated Systems* (*AFQRJOS*), Bulletin No. 4, Issue 20, March 2005; www.paclp.com/profile/releases/AFQRJOSIssue20.pdf.
(38) Service Des Essences Des Armées, Direction Centrale, Ministère De La Défense, *Guide technique des produits distribués par le SEA*; 2006/2007 ed.; www.defense.gouv.fr/essences/content/download/41978/420611/file/guides_techniques_gtp_2006_2007.pdf.
(39) Edwards, T; Maurice, L. Q. *J Propul Power* **2001**, *17*, 461–466.
(40) Bikas, G.; Peters, N. *Combust. Flame* **2001**, *126*, 1456–1475.
(41) Buda, F.; Battin-Leclerc, F.; Glaude, P. A.; Conraud, V.; Bounaceur, R. Modèle Cinétique Unifié pour la Simulation de l'Auto-Inflammation des Alcanes. *Journée des Doctorants en Combustion 2004 Groupement Français de Combustion*; http://www.gfcombustion.asso.fr/jdoc/jd2004-buda.pdf.
(42) Mawid, M. A.; Park, T. W.; Sekar, B.; Arana, C.; Aithal, S. M. *Development of a Detailed Chemical Kinetic Mechanism for Combustion of JP-7 Fuel*; AIAA: 2003−4939
(43) Catoire, L.; Swihart, M. T.; Gail, S.; Dagaut, P. *Int. J. Chem. Kinet.* **2003**, *35* (9), 453−463.
(44) Dagaut, P.; Bakali, A. El; Ristori, A. *Fuel* **2006**, *85*, 944–956.
(45) Dagaut, P.; Cathonnet, M. *Prog. Energy Combust. Sci.* **2006**, *32*, 48–92.
(46) Yan, S.; Eddings, E. G.; Pugmire, R. J.; Sarofim, A. F. *Formulation and Some Applications of Jet Fuel Surrogates*. Conference C-SAFE, Department of Chemical & Fuels Engineering University of Utah: 2004. http://www-acerc.byu.edu/News/Conference/2004/Presentations/Shihong%20Yan.pdf.

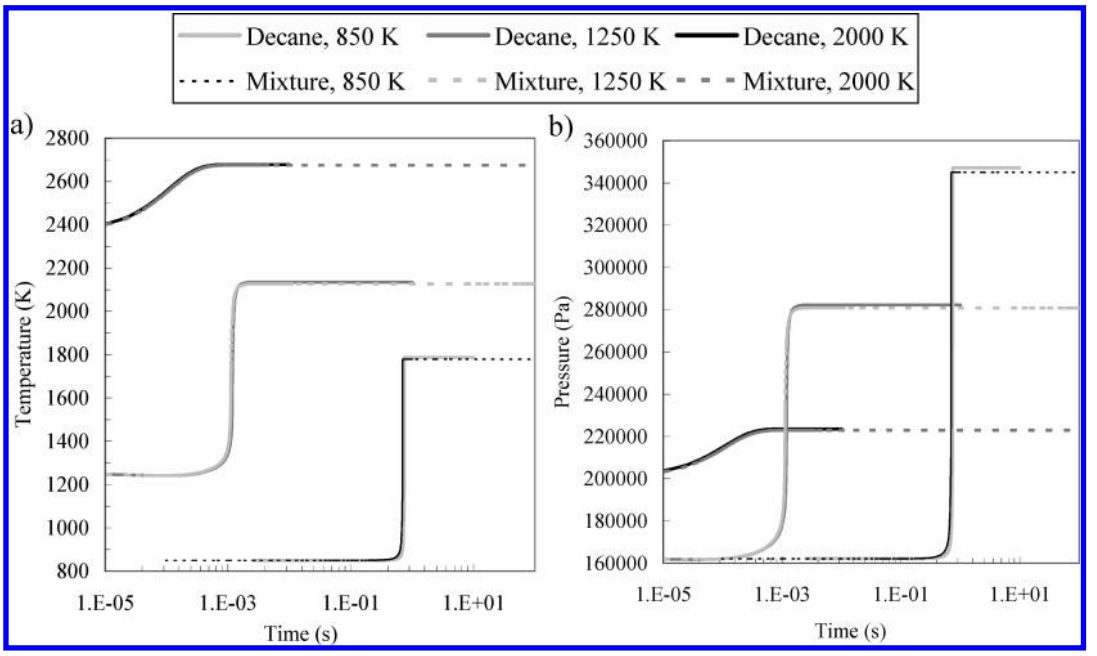

Figure 1. Temperature (a) and pressure (b) evolution during combustion of two kerosene surrogates for three initial thermal loading.

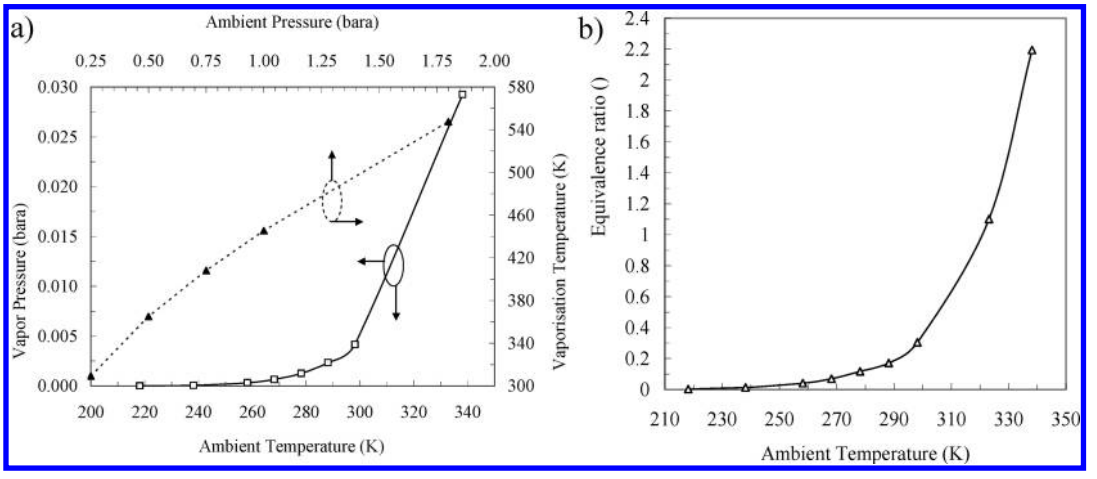

Figure 2. Decane gaseous vapor pressure and vaporisation temperature (a) with corresponding equivalence ratio in air (b).

Table 1. Ignition Delay and Maximum Rate of Pressure Rise of Two Kerosene Surrogates at Different Initial Thermal Loading

	ignition delay (s)			maximum rate of pressure rise (bar·s^{-1})		
initial temperature (K)	850	1250	2000	850	1250	2000
decane	7.43×10^{-1}	1.18×10^{-3}	1.04×10^{-5}	3.38×10^{8}	3.37×10^{9}	3.99×10^{9}
mixture of 3 components	7.0×10^{-1}	1.12×10^{-3}	1.02×10^{-5}	1.38×10^{8}	2.87×10^{9}	4.01×10^{9}

where T_C and P_C are the critical temperature and pressure, and P_{atm} is the atmospheric pressure.

The data are represented for the decane in Figure 2a. Depending on the ambient temperature, the equivalence ratio is expressed based on the saturation pressure (Figure 2b). The lower flammable limit (LFL) and the upper flammable limit (UFL) are, respectively, 0.8 and 5.4 vol % for the decane. These values correspond to an equivalence ratio of 0.595 and 4.212, thus a temperature range of 310−353 K (Figure 2b). Nevertheless, the minimum temperature that will be considered is 298 K to observe the phenomenon at ambient conditions. The maximum temperature is related to the conditions that are encountered by an air system; that is to say about 338 K. The pressure range corresponds to the air system pressurization is 1−1.8 bara.

2.3. Use of Detailed Chemistry for the Establishment of a Global Kerosene Combustion Law. The decane combustion mechanism of Dagaut and Cathonnet[45] has been first used to propose a one-step global Arrhenius law that could be used in another kerosene tank compartments simulation.[47] This law is based on the formulation proposed by Najjar and Goodger (eq 3).[48] In their studies, the coefficients have been established to describe the fuel combustion in

(47) Pascaud, J. M.; Gillard, P.; Gascoin, N. *Simulation of the combustion of kerosene vapors by a multi-physics model*; 22th ICDERS, Minsk (Belarus), July 27−31, 2009.
(48) Najjar, Y. S. H.; Goodger, E. M. *Fuel* **1981**, *60*, 980–986.

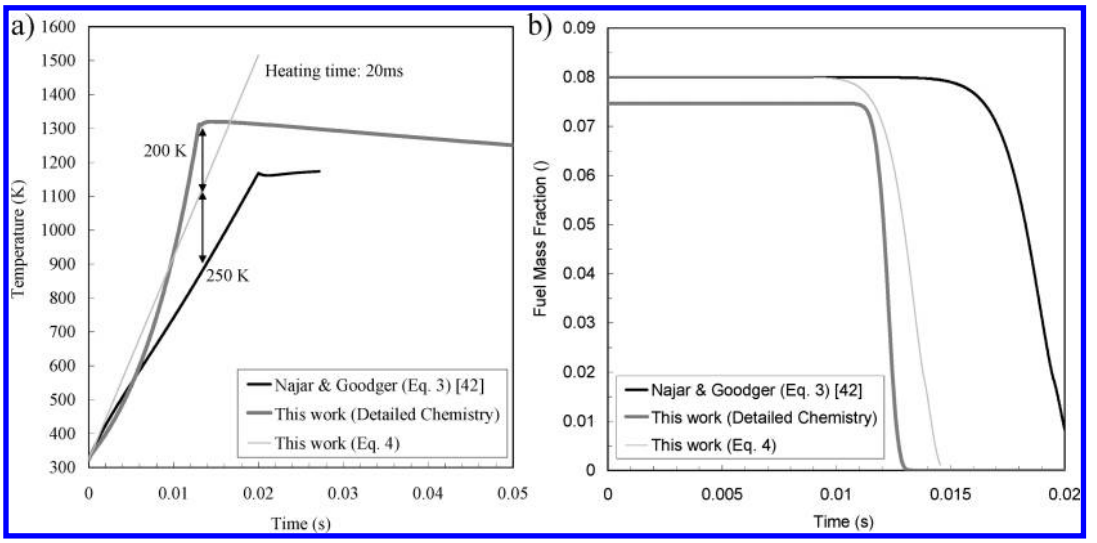

Figure 3. Temperature increase (a) and kerosene consumption (b) comparison between detailed kinetics and two global combustion laws.

turbo-machinery configuration. The pre-exponential factor has been modified (8×10^6) by Aly and Salem[49] to correctly predict the laminar burning velocity.

$$\dot{\omega} = -\frac{\mathrm{d}[\mathrm{HC}]}{\mathrm{d}t} = (2 \times 10^6) \times P^{0.3} \times T \times [\mathrm{O_2}] \times [\mathrm{HC}]^{0.5} \times \exp(-13600/T) \quad (3)$$

By comparison with the decane detailed combustion mechanism,[45] the Najjar and Goodger formulation is the most suitable one around a temperature of 1000 K, while that of Aly and Salem is most suitable around 1500 K. Nevertheless, both are not adapted under 1000 K, and they can easily underestimate the temperature by 300 K. This is a strong drawback to well describe the initiation. Thus, two sets of parameters have been proposed: one under 950 K (eq 4) and one above 1250 K (eq 5). The formulation of Najjar and Goodger could still be used in the range 950−1250 K.

$$\dot{\omega} = -\frac{\mathrm{d}[\mathrm{HC}]}{\mathrm{d}t} = (8.2 \times 10^7) \times P^{0.3} \times T \times [\mathrm{O_2}]^{0.15} \times [\mathrm{HC}]^{0.72} \times \exp(-23500/T) \quad (4)$$

$$\dot{\omega} = -\frac{\mathrm{d}[\mathrm{HC}]}{\mathrm{d}t} = (6 \times 10^4) \times P^{0.3} \times T \times [\mathrm{O_2}]^{0.5} \times [\mathrm{HC}]^{0.3} \times \exp(-20000/T) \quad (5)$$

The "low temperature" formulation proposed in this paper (eq 4) is compared to the one of Najjar and Goodger and to the detailed chemistry (Figure 3a). The reactive mixture is heated for 13 ms. At this time, the low temperature formulation presents a thermal underestimation of 200 K, whereas the Najjar and Goodger law underestimates the temperature by 450 K. This is qualitatively interesting for eq 4, but this also shows its limit, which is coped by with eq 5. The temperature increase between 13 and 20 ms is due to the longer applied heat flux. The underestimation by the proposed formula could also be due to a low heat release and not due to the fuel consumption speed. Indeed (Figure 3b), the kerosene conversion presents a good agreement in comparison with detailed chemistry, better than the one of Najjar and Goodger.[48] Nevertheless, the necessity to consider the detailed chemistry into account is clearly visible in this subsection.

2.4. Choice of the Numerical Code. The well-known CHEMKIN package has been considered with the SENKIN program, the 0D static reactor configuration, to observe its ability to characterize the involved phenomenon. The initiation is provided by a temperature increase. If the results are suitable to estimate an ignition delay or an explosion severity, for example, it is difficult to link the results to a real configuration. Indeed, the ignition by an overall temperature increase is not appropriate to describe a local initiation, or even multipoint. Furthermore, the code always considers one mole of mixture. For a fixed initial pressure, the thermal rise corresponds to a volume decrease due to the perfect gases law. SENKIN cannot represent the pressure increase that is linked to the mole number elevation. Consequently, the SENKIN program cannot face the initiation of kerosene vapor explosion.

The single point, which can be verified with SENKIN, is qualitative. In particular, the final temperature after explosion is linked to the initial one (Figure 4a). For lean mixtures, the higher the equivalence ratio, the higher the temperature. This is also visible on the test case with an initial temperature of 2000 K, for which the maximum reached temperature is plotted versus the equivalence ratio. The initial pressure does not impact on the thermal aspect (Figure 4a) but only on the pressure (Figure 4b). The maximum pressure increases when the equivalence ratio rises and when the temperature decreases. This latest point is due to the limitation of SENKIN because of the constant mole number assumption and because of the initiation by the overall volume heating.

Several other codes, dedicated to gas explosions, can be found in literature. The most famous and important one is probably the FLACS (FLame ACceleration Simulator) code.[50] It has been extended to dust explosion in the framework of the European DESC (dust explosion simulation code) project.[51] FLACS is a CFD (computational fluid dynamics) code, which is based on experimental data from a chemical point of view. Thus, it uses combustion parameters deduced from pressure-time histories measured in spherical closed vessel of 20 L. The local burning velocity is

(49) Aly, S. L.; Salem, H. *Fuel* **1989**, *68*, 1203–1209.

(50) Middha, P. *J. Loss Prev. Process Ind.* **2009**, doi:10.1016/j.jlp.2009.07.020.

(51) Skjold, T. *J. Loss Prev. Process Ind.* **2007**, *20*, 291–302.

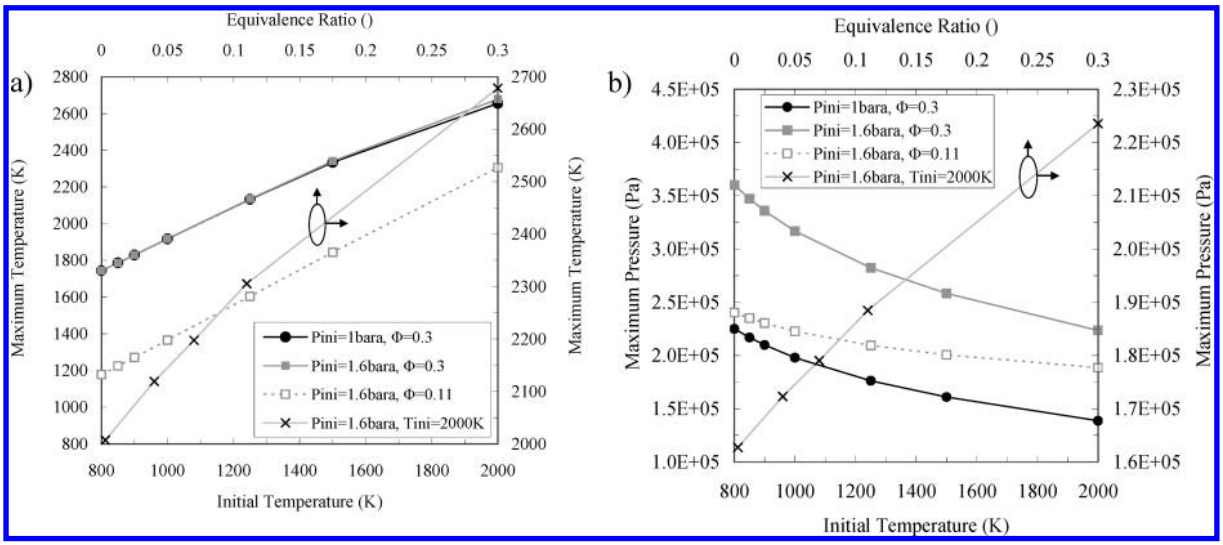

Figure 4. Explosion temperature (a) and pressure (b) computed with SENKIN for several initial pressures, temperatures, and equivalence ratios.

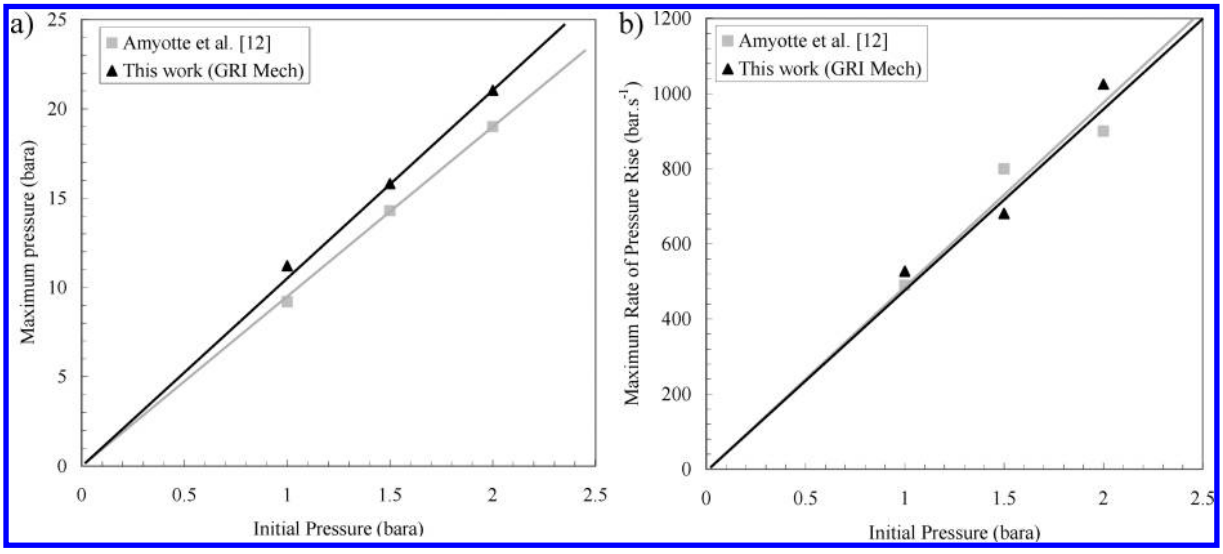

Figure 5. Explosion pressure and severity of ethylene−air stoichiometric mixture computed with MIRAGE.

computed by empirical laws and the flame thickness by the β flame model.[51] These data are obtained for propagating flames with constant parameters and not for transient conditions from the beginning of the ignition (no consideration of complex phenomenon due to energetic ignition sources and wall effects). Despite an empirical law, which is employed to correct this drawback; the behavior of FLACS in transient conditions still requires improvements. The results are notably grid dependent for the initial ignition phase.[51] FLACS considers a complete combustion that may not be appropriate to the present study. A thermodynamic equilibrium approach is also considered, while the kinetic modeling of the reactive fuel is of prior importance in the present study due to the two-steps mechanism (pyrolysis of the initial hydrocarbon fuel followed by the combustion of the byproduct). Concerning the fluid flow, the turbulence flame velocity is considered through an empirical equation.[51] FLACS better describes the fluid mechanics than the chemistry (both cannot be considered accurately due to the computational cost). This is nevertheless a very interesting numerical tool for gas and dust explosions encountered in the framework of safety studies, notably for very large configurations (few meters of characteristic length). It allows considering building and obstacles.[53]

2.5. Presentation of the Numerical Code MIRAGE. The numerical tool MIRAGE is based on the 1D RESPIRE code,[54] which aimed at studying reactive flows in open-end channel configuration. The Navier−Stokes equations are discretized in space with finite difference centered scheme and explicitly time-solved as ordinary differential equations with the Runge−Kutta 4 method. The energy and transport equations are considered with the detailed chemistry. The equations that are present in the code are extensively detailed in previous work.[54,55]

If using the MIRAGE code in full 1D configuration, a space step of 1 mm to 1 cm with adapted Courant−Friedrichs−Lewy condition is acceptable without degrading the

(52) Klemens, R.; Zydak, P.; Kaluzny, M.; Litwin, D.; Wolanski, P. *J. Loss Prev. Process Ind.* **2006**, *9*, 200–209.

(53) Hanna, S. R.; Hansen, O. R.; Dharmavaram, S. *Atmos. Environ.* **2004**, *38*, 4675–4687.

(54) Gascoin, N.; Gillard, P.; Bernard, S.; Daniau, E.; Bouchez, M. *Int. J. Chem. React. Eng.* **2008**, *6*, A7.

(55) Gascoin, N.; Gillard, P.; Dufour, E.; Touré, Y. *J. Thermophys. Heat Transfer* **2007**, *21*, 86−94.

accuracy of the results. This configuration presents the main interest to study the ignition location and multipoint ignition effects. Unfortunately, the computational cost makes it impossible to be used for intensive parametric study for the vulnerability purpose. Thus, the code has been adapted to the present closed configuration, which is modeled as follow. A small ignition volume of 1 cm^3 or less is considered inside the kerosene tank and a heat flux is applied on it for a time of several milliseconds. This volume numerically represents one computation cell while the reactive mixture under study is another c ell. No physical boundary exists between these volumes. The ignition is located on the side of the reactive mixture. The size of this small initiation cell and the energy resulting from the heat flux can be varied to conduct a parametric study.

The MIRAGE code has been validated by comparison with gaseous explosions data from the literature. For example, the data from Amyotte et al.[13] on a 26 L spherical closed vessel filled with stoichiometric ethylene−air mixture are presented (Figure 5). The GRIMECH combustion mechanism is used specifically for this validation because the one of Dagaut and Cathonnet[45] is not dedicated to ethylene−air mixture. The 138 J experimental energy is applied on a volume of 125×10^{-9} m^3 (cube side of 5 mm) during 50 ms. The pressure reached after explosion is slightly higher with MIRAGE. It can be due to the chemical mechanism (Figure 5a). This remains acceptable for a safety studies because, first, it overestimates the maximum pressure, and, second, the discrepancies are lower than 10%, which is acceptable due to experimental uncertainties. The resulting explosion severity deduced from calculations is close to the experimental one (Figure 5b).

For the same conditions, another calculation with only 35 J did not allow observing explosion, wehreas at 45 J the explosion arises. This can be a way of estimating the spark igniter efficiency, for example, around 35/138 to 45/138, that is to say 25.4−32.6%.

The MIRAGE and the FLACS codes can be briefly compared. FLACS appears to be largely adaptable to a wide variety of real configurations (offshore platforms, gas sprays, liquid hydrogen release, etc.). It is a three-dimensional code that is largely supported by universities and companies in Europe. A large number of validations are conducted to enhance its behavior. MIRAGE is mostly suitable for the application to which it is proposed, that is to say the kerosene explosions in closed vessel. But the main advantage of MIRAGE is to consider the detailed chemical mechanisms of the pyrolysis and of the combustion of the fuel involved in the explosion process. The coupling between the combustion, the expansion of burned gas, the gas flow, and the chemical rate is taken into account. The Navier−Stokes equations consider the turbulent flow with empirical correlation, and the transport equation of chemical species allows considering the coupling between fluid mechanics and chemistry.

Finally, because this work may be considered as a part of an engineering program aiming at estimating the impact of explosion on a kerosene tank, MIRAGE is judged to be an interesting tool. Of course, it cannot be used to study the flame propagation and overpressure development in compartments, but it is of major interest for the initiation, which is the first step in safety studies. Although CFD calculations would be better, it is obvious that with detailed chemistry it is difficult to conduct parametric studies on a tank of several cubic meters with flame thickness on the order of 1 mm^3.

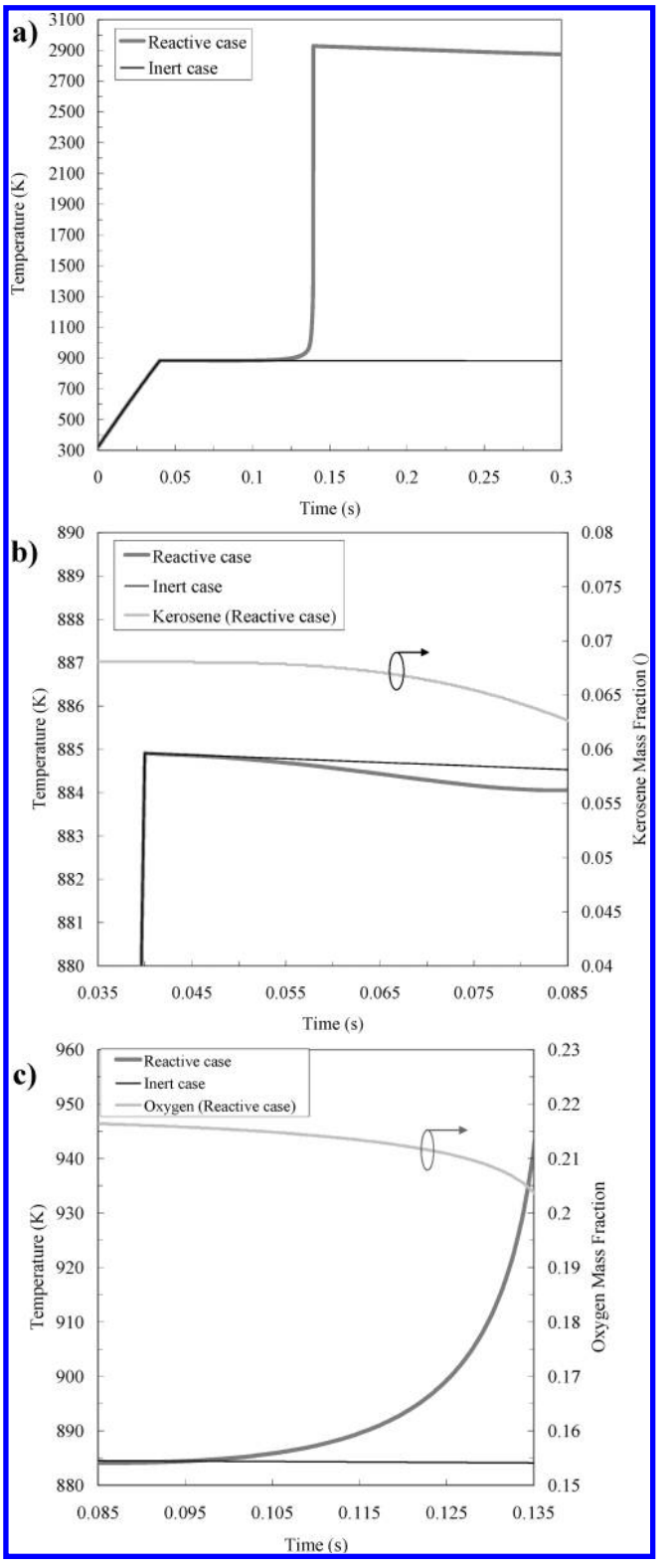

Figure 6. Temperature increase (a) with related composition of fuel (b) and oxygen (c) for reactive and nonreactive test cases.

3. Characterization of Kerosene Explosion

The explosions of kerosene vapors in one compartment tank are studied through a parametric study by varying the

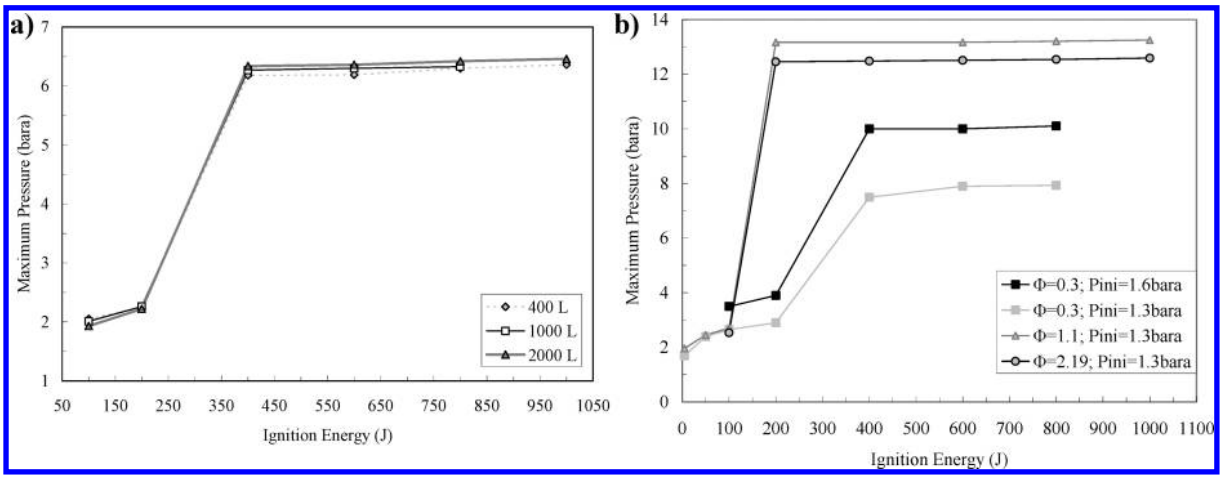

Figure 7. Ignition energy dependence of the maximum pressure computed for: (a) three volumes (initial pressure of 1.3 bara, equivalence ratio of 0.3) and (b) several equivalence ratios and initial pressures (volume of 1 m^3).

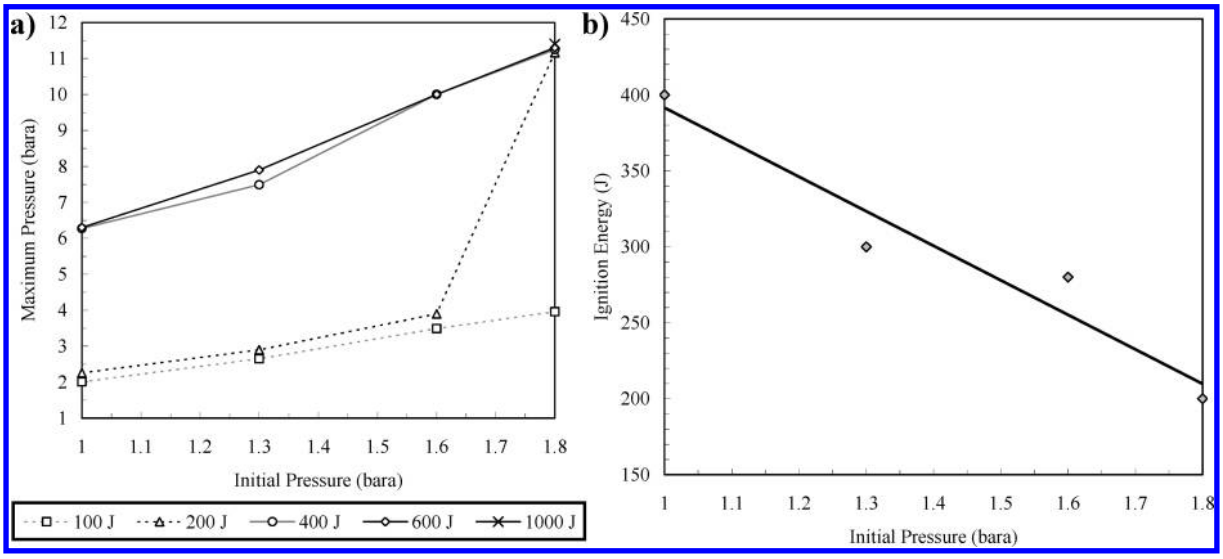

Figure 8. (a) Maximum pressure after explosion depending on initial pressure for several ignition energies (equivalence ratio of 0.3, volume of 1 m^3); (b) initial pressure dependence of the ignition energy (volume of 1 m^3, equivalence ratio of 0.3).

volume of the tank, the ignition energy, and the initial temperature and pressure (thus the equivalence ratio). The gathered data are the temperature and pressure increase, their maximum value, and the explosion severity. An example is given between a reactive (kerosene−air) and a non reactive (nitrogen) case to underline the efficiency of the code to observe the initiation mode. During the first 40 ms initiation step (Figure 6a), both cases present a thermal increase. Then, while nothing noticeable appears for the inert case, the reactive one presents a chemical induction delay of about 8 ms before a sudden explosion for which the temperature reaches 2800 K. Indeed, a first endothermic step of kerosene decomposition is observed (Figure 6b) before an exothermic step of pyrolysis products combustion with O_2 consumption (Figure 6c).

The numerical results for MIRAGE allow proposing an explosion model to estimate the related severity depending on the conditions. Empirical laws will be proposed to be implemented in the ALBAS software.

3.1. Definition of the Computation Parameters. There are several ignition methods: sparks, hot wires, exploded wires, heated surfaces, pilot flames, pyrotechnic igniters, laser sources, etc. The ignition by one or more projectile may be different because the phenomenon could be linked to a shock wave generation due to the supersonic hot ammunition speed, as seen in Section 1. It has been chosen in the MIRAGE code to apply a heat flux into an ignition cell. This small volume and the duration of the heat flux application can be varied independently. This configuration is representative of an electric spark ignition. After several trials, an ignition volume is arbitrarily fixed to the value of 1 cm^3 because it is in the order of the size of a projectile. This volume can be changed if necessary (see Section 2.5) to adapt the code to a specific test configuration. The duration is fixed depending on the energy. Indeed, the applied heat flux is constant and equal to 10 $GW \cdot m^{-3}$. This flux is generally the maximum one that is accepted by the MIRAGE code to avoid numerical divergence with reasonable time step (even if some calculations have been done with 20 $GW \cdot m^{-3}$). This also ensures a security range on the results because decreasing this heat flux for the same energy could only diminish the explosion probability. The duration of the energy deposition is a consequence. The position of the ignition cell in the reactive mixture is not studied in this paper despite the strong influence of the ignition location. Numerous studies of literature are available to cover this point.[14] But because

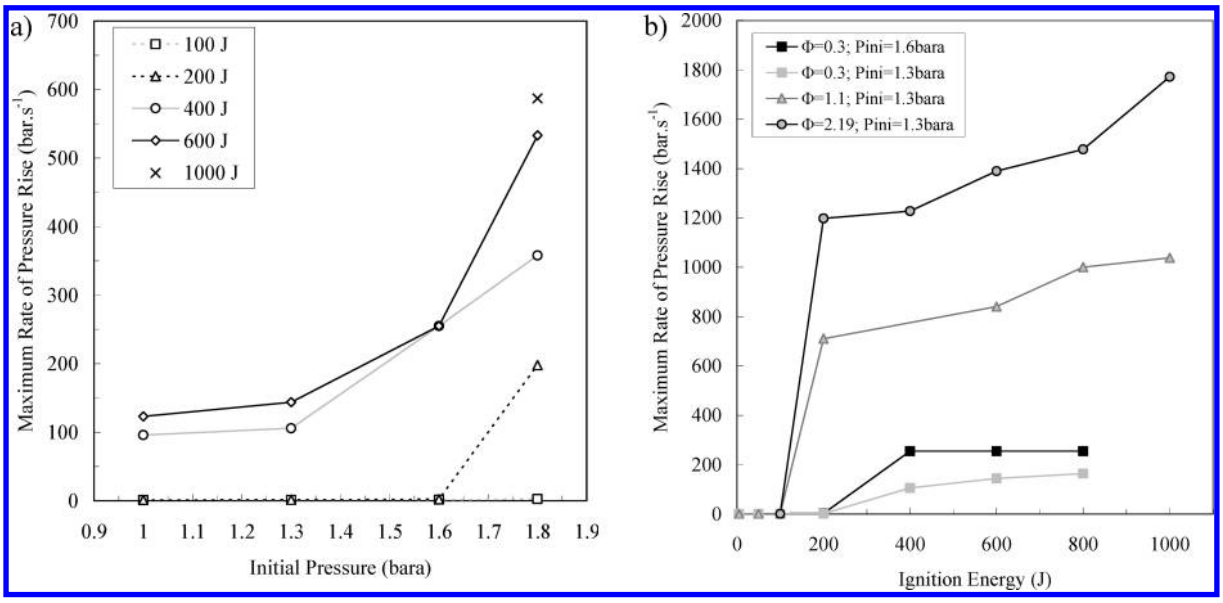

Figure 9. Dependence of the explosion severity on initial pressure for an equivalence ratio of 0.3 (a) and on ignition energy for several equivalence ratios and initial pressures (b).

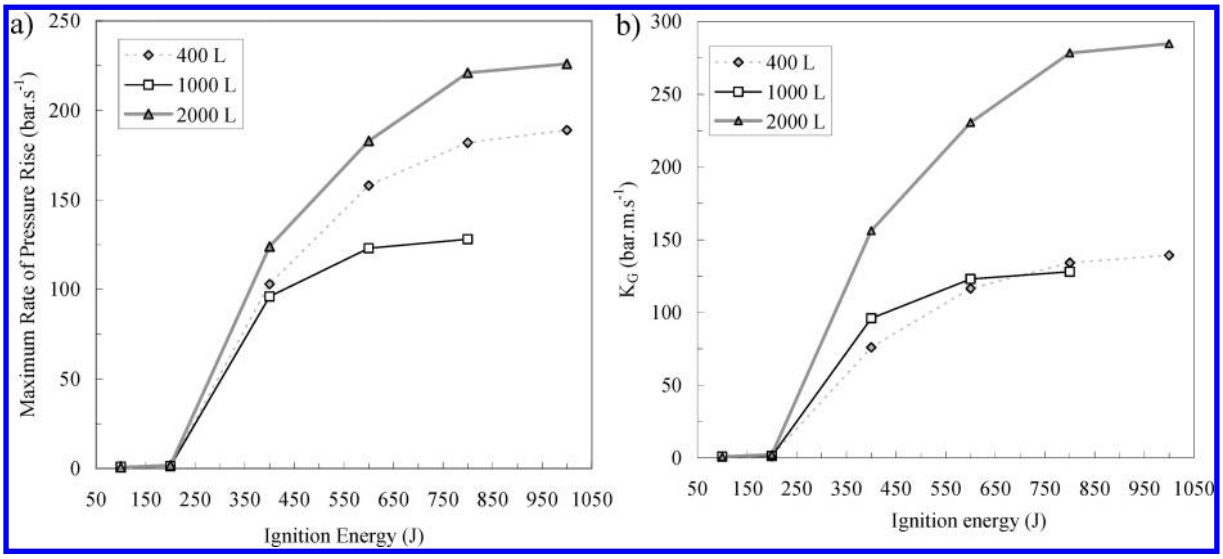

Figure 10. Maximum rate of pressure rise (a) and related K_G values (b) for three volumes (Equivalence ratio of 0.3 and initial pressure of 1 bara).

the real ignition way is multipoint and very difficult to handle, it was chosen in this first approach of kerosene explosion to not study in details the ignition and the location influence.

3.2. Results of MIRAGE Computations. The maximum pressure that is reached after explosion is plotted for three cubic volumes of kerosene tank depending on the applied energy (Figure 7a). The volume does not impact this pressure, but it depends first on the ignition energy (thus the heat flux duration), second on the equivalence ratio, and third on the initial pressure (Figure 7b). For an equivalence ratio of 0.3, no explosion appears under 200 J and the peak pressure is only due to the heating. Numerically, the explosion appears at 400 J because no energy has been tested in this range. This curve shape is kept voluntary and the exact energy, above which the explosion occurs, is not of interest. Indeed, this sigmoid shape is more appropriate to represent real ignition conditions. The numerical simulation is determinist. For a given energy, go or no go explosion is defined. Experimentally, this energy is called E_{50} and it represents the 50% probability to have an explosion. This parameter is frequently used in safety studies. The sigmoid shape represents this fuzzy boundary between explosion and no explosion.

This maximum final pressure is proportionally linked to the initial one (Figure 8a) for energies generally over 200 J; while no explosion occurs under 200 J (except for the case of 1.8 bara initial pressure). For this latest specific case, the combined effect of pressure and energy is shown. This phenomenon is well-known and it is sometimes represented with a power law giving the ignition energy as a function of the pressure.[4] As seen in Section 2, the higher the initial pressure, the higher the explosion pressure (and temperature because of perfect gases law). Thus, for the same energy level, the temperature in the ignition cell increases slightly with the initial pressure rise. When approaching the ignition temperature, this can be sufficient to get an inflammation in the overall kerosene tank. This is the reason why the initial

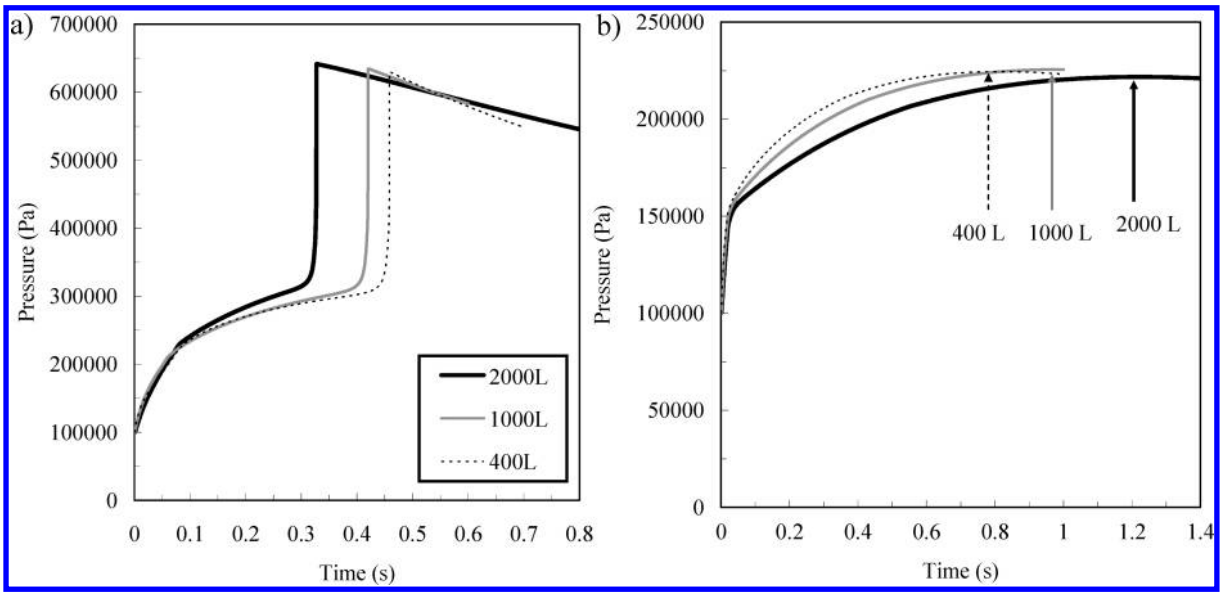

Figure 11. Pressure dynamic for three volumes with (a) and without (b) explosion at respectively 800 and 200 J.

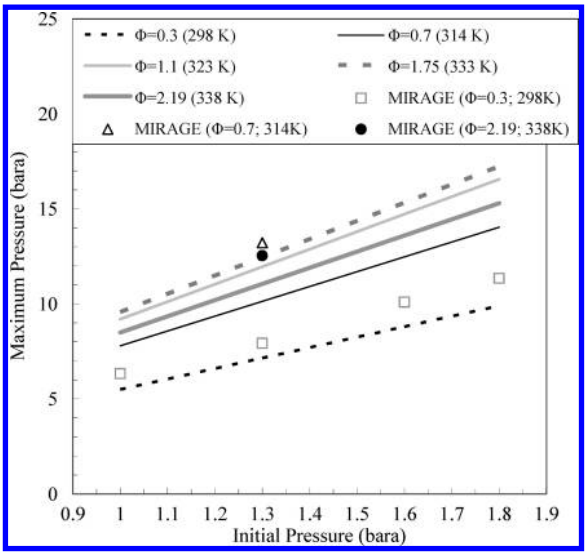

Figure 12. Linear relationship between final and initial pressures for several equivalence ratios (analytical law of eq 6 given by lines and MIRAGE results given by symbols).

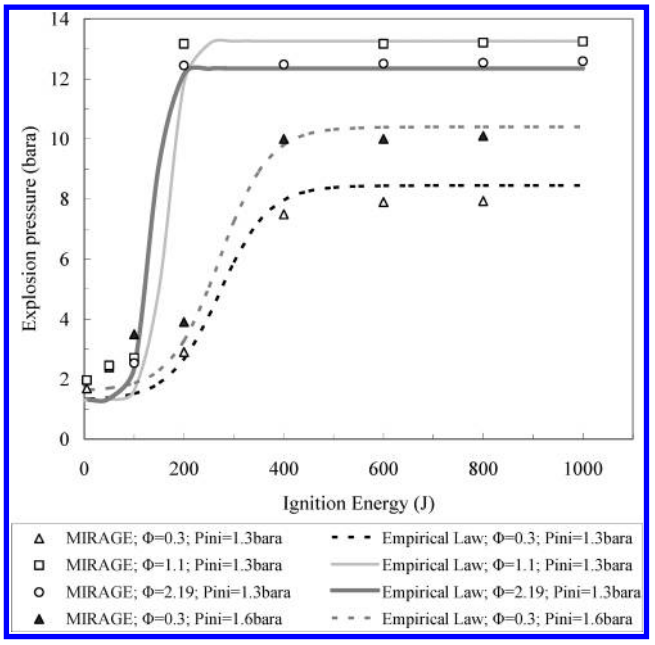

Figure 13. Explosion pressure obtained by empirical law and numerical simulation as a function of ignition energy.

pressure plays a role in the initiation process and can impact on the ignition energy (Figure 8b).

The explosion severity can also be plotted as a function of initial pressure (Figure 9a) or of ignition energy (Figure 9b). In particular, the 200 J threshold and the coupling between the energy and the initial pressure are visible (Figure 9a). In terms of the explosion dynamics, the equivalence ratio plays a major role, and this is one of the most important points to estimate the explosion severity.

The time derivative of the pressure is also a function of the volume (Figure 10a) because for an established flame propagation, the bigger the volume, the longer the time to reach an equilibrium. Nevertheless, the results of the 0.4 m^3 are comprised between those of the two biggest volumes. When computing the corresponding K_G values, the 0.4 and 1 m^3 volumes present very similar values, whereas the 2 m^3 tank has a specific behavior (Figure 10b). The K_G is considered to be mostly applicable up to 200 bar·m·s^{-1};[56] so the 2 m^3 volume should be considered carefully because it presents values up to 300 bar·m·s^{-1}. Furthermore, the K_G is known to be different depending on the geometry of the enclosure.[8] For the same volume, a spherical shape and a cubic one for example will present different values while they have the same cubic root of the volume. So, the characteristic geometric length should be more suitable to compute the K_G (for example the diagonal of the cube). For a large variation of the volume of the vessel, the K_G can even vary from a factor 2 as observed in literature.[8]

This difference between the tank sizes is attributed to a competitive effect between the flame speed and the tank volume. Indeed, for a small volume, the flame rapidly

(56) Eckhoff, R. *Dust Explosions in the Process Industries*, 3rd ed.; Elsevier Science: USA, 2003; ISBN: 978−0-7506−7602−1.

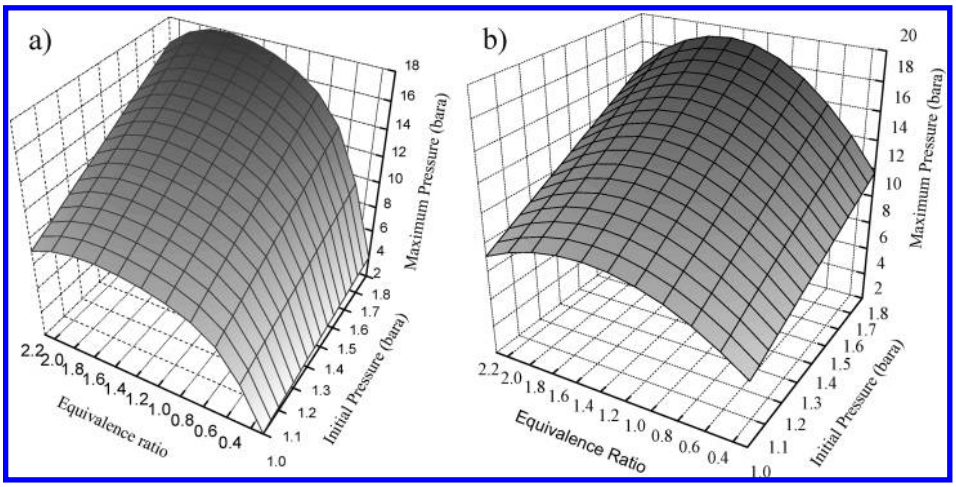

Figure 14. Representation of explosion pressure depending on the initial pressure and equivalence ratio at 200 J (a) and 800 J (b) for a volume of 1 m^3.

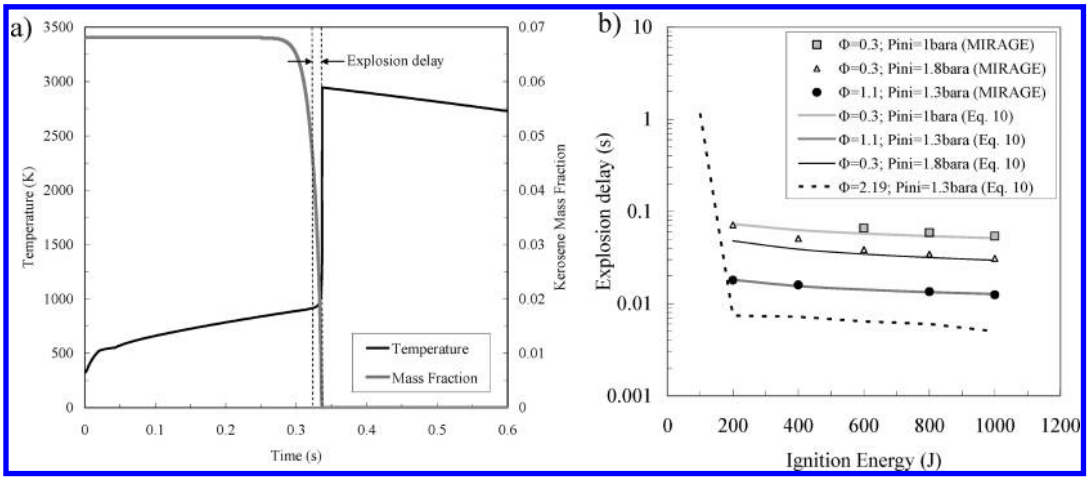

Figure 15. Explosion delay measured on numerical curve (a) and plotted vs energy for several equivalence ratios and initial pressures (volume of 1 m^3) to be compared with empirical law (b).

reaches the boundary and the dynamic of the explosion is relatively fast (small volume on surface ratio). Increasing the size of the volume first slows down the dynamic because the volume is not sufficient to propagate freely. Then for even bigger geometric sizes, the flame accelerates due to the turbulence (as mentioned in Section 1.1). When the volume to surface ratio of the tank is high enough, the propagation of the flame reaches its established regime. Increasing the volume again makes the dynamic of the explosion to be finally reduced. This is illustrated by one case at 800 J (Figure 11a) for which the fastest dynamic corresponds to the biggest volume while the dynamic at 200 J (Figure 11b), without flame propagation but only thermal convection, is much slower for the bigger tank.

3.3. Estimation of the Maximum Pressure As a Function of the Initial One. On the basis of these MIRAGE results, several empirical laws have been proposed. First, the maximum pressure can be simply given depending on the initial one as follows. The proportionality coefficient is expressed as a function of Φ the equivalence ratio in relationship with Figure 7. Thanks to its parabolic formulation, this coefficient presents a maximum for slightly rich mixtures, which is physically accepted. At largely lean or rich mixture, the air or the fuel, respectively, act as diluents and moderate the explosion pressure. The maximum pressure given by the analytical formula is plotted with lines versus the initial pressure and compared for several equivalence ratios to the one (symbols) computed by MIRAGE (Figure 12).

$$P_{\max} t = \alpha P_{\text{ini}} \tag{6}$$

$$\alpha = -2.7869\Phi^2 + 8.5266\Phi + 3.1928 \tag{7}$$

But eq 6 does not evaluate if the explosion will occur or not because the ignition energy is not considered. So, the following expression (eq 8) is proposed. A sigmoid law is used because of the curve shape obtained in Figure 7. The explosion pressure is at least equal to the initial one, and it tends to the maximum one given by the eq 6 depending on the energy. To represent the energy threshold, which is shifted toward high energy when decreasing the equivalence ratio, a minimum energy is considered. It corresponds to the minimum value that should be supplied to the ignition volume to propagate the flame. The ratio of the maximum pressure on the initial one lets appearing the proportional coefficient of eq 7.

$$P_{\text{exp}l} = P_{\text{ini}} + \frac{P_{\max}}{1 + \exp\left(-\frac{E}{E_{\min}} + \frac{P_{\max}}{P_{\text{ini}}}\right)} \tag{8}$$

$$E_{\min} = (0.2\Phi^{-2} + 1)\Delta H_{\text{comb}} m_{\text{carb}} \tag{9}$$

The curves obtained thanks to this analytical formula have been compared to the data obtained by numerical

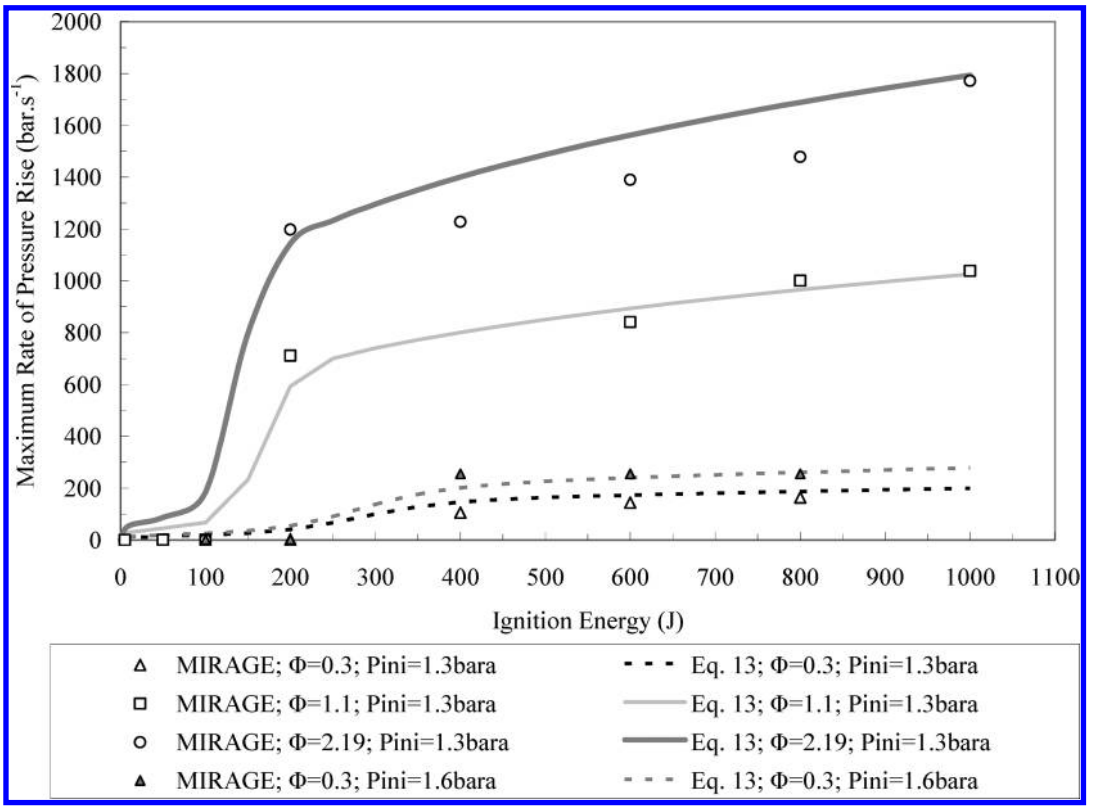

Figure 16. Explosion severity of 1 m^3 volume, or K_G, at different pressures and equivalence ratios: comparison between MIRAGE results and empirical law.

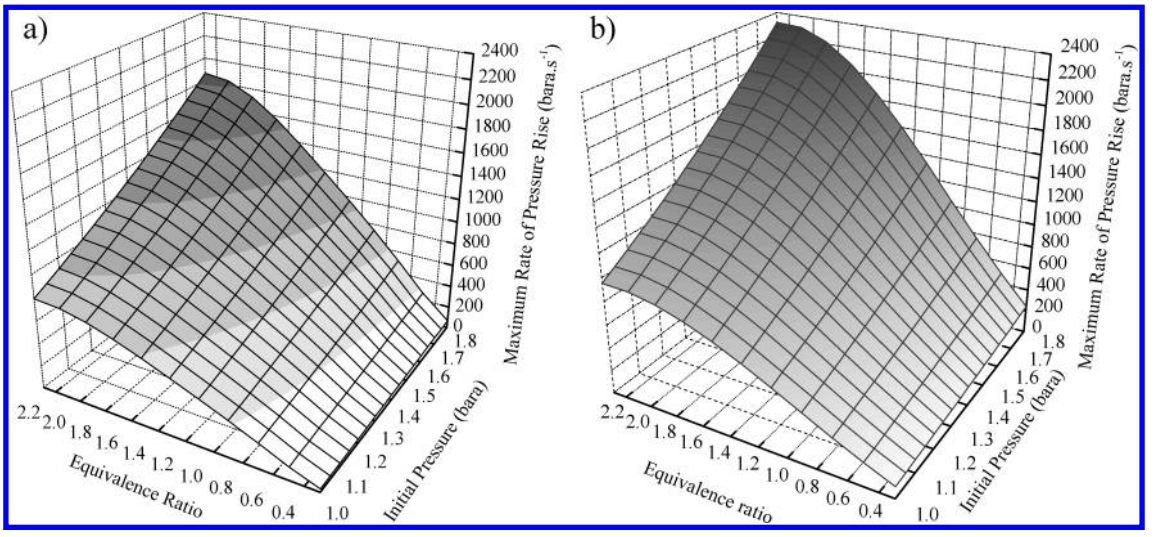

Figure 17. Representation of maximum rate of pressure rise depending on the initial pressure and equivalence ratio at 200 J (a) and 800 J (b) for a volume of 1 m^3.

simulation (Figure 13). The agreement is correct and it is judged to be acceptable in the framework of the air system vulnerability. This represents a first step in the consideration of vapor explosions by global laws. The analytical formula (eq 8) is also represented in Figure 14 for two energies. The dependency of the explosion pressure on the three main important parameters is visible.

3.4. Estimation of Explosion Delay. The explosion delay corresponds in this study to the time required to convert half of the fuel quantity (Figure 15a). The entire time of consumption is not considered because of the first endothermic pyrolysis step that precedes the combustion reaction (Figure 6). The delay (of which unit is in second (s) if the parameter b is equal to 1) is expressed as a function of the ignition energy (eq 10) with a factor A (eq 11). This latest is used to take several phenomena into account. The competitive effect between the flame propagation and acceleration and the volume typical length (its cubic root) is considered at the numerator. The denominator is the minimum heat flux to elevate the ignition volume of about 400 K (typical thermal increase to consider that an ignition occurs). The factor A is inversely proportional to the equivalence ratio

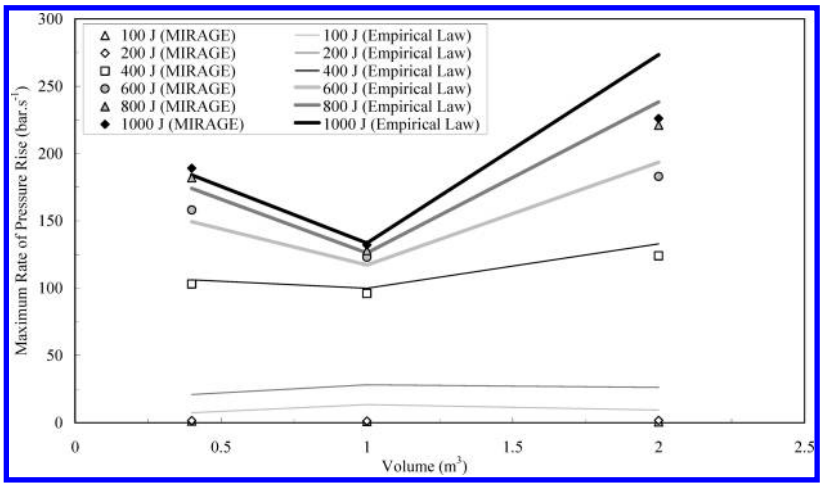

Figure 18. Volume dependency of the explosion severity observed on numerical simulation results (points) and approached by empirical formulas (lines).

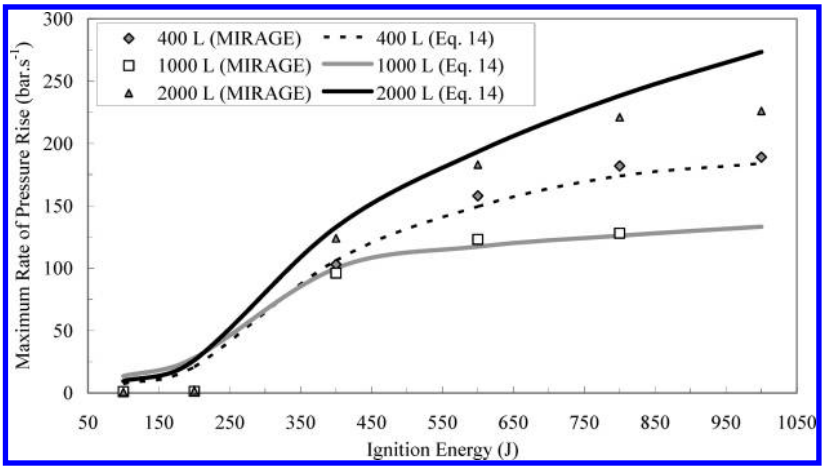

Figure 19. Empirical laws compared to numerical simulations with MIRAGE on maximum rate of pressure rise for several volumes (initial pressure of 1 bara and equivalence ratio of 0.3).

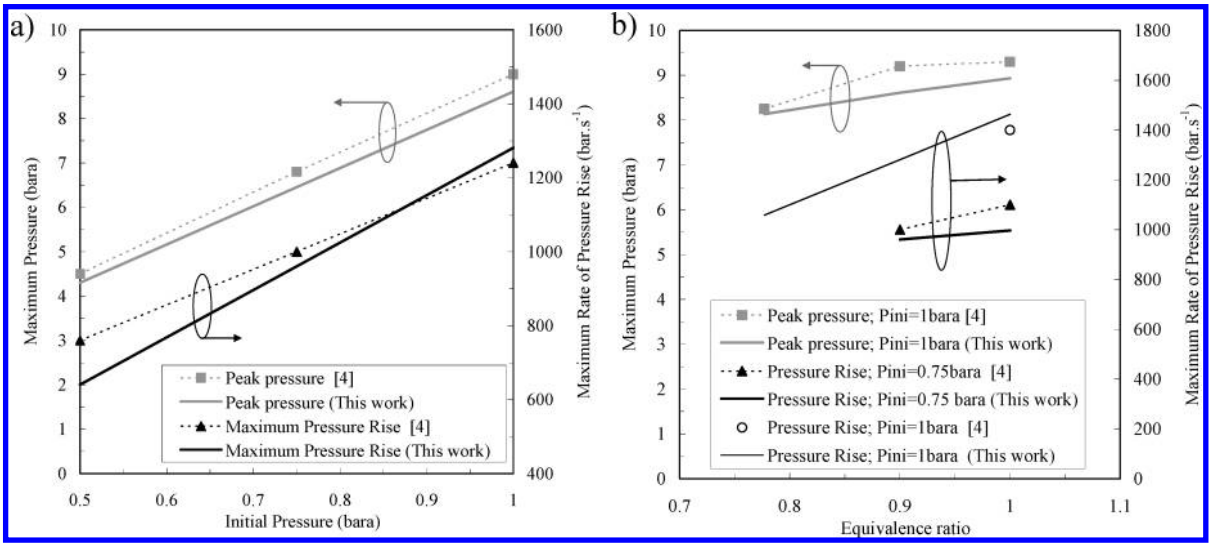

Figure 20. Kerosene vapor explosions investigated by empirical laws and compared with experimental propylene-air mixtures results[5] as functions of initial pressure for an equivalence ratio of 0.9 (a) and as functions of equivalence ratio for two pressures (b).

to decrease the explosion delay when the equivalence ratio increases. The exponent b in eq 10 is given under a second order polynomial form (eq 12), which depends on the nondimensional initial pressure (divided by the atmospheric one). The resulting empirical law (eq 10) is plotted and compared to MIRAGE results (Figure 15b). The agreement is

judged to be satisfactory despite the discrepancies for lower energies.

$$\tau_{expl} = AE^b \tag{10}$$

$$A = \frac{\frac{\mathrm{vol}^{1/3}}{S_u}}{\mathrm{m_{carb}} C_p.\Delta T} \Phi^{-0.9149} \tag{11}$$

$$b = 0.0083\left(\frac{P_{ini}}{P_{atm}}\right)^2 - 0.0858\left(\frac{P_{ini}}{P_{atm}}\right) - 0.1725 \tag{12}$$

where vol is the tank volume, S_u the laminar flame speed (0.45 m.s^{-1} for the kerosene), m_{carb} is the mass of kersone in the initiation cell, C_p is the heat capacity of the reactive mixture, and ΔT is the thermal increase generally admitted for an ignition, that is to say 400 K.

3.5. Estimation of Explosion Severity for a Volume of 1 m^3, the K_G. The explosion severity is proposed (eq 13) by simply dividing the previous empirical law concerning the maximum pressure (eq 8) by the explosion delay (eq 10). For a 1 m^3 volume, the calculated pressure time derivative is equal to the K_G value because of the unitary volume. It is compared to numerical simulations (Figure 16). The agreement is acceptable. Equation 13 is represented for two energies depending on the initial pressure and temperature, thus the equivalence ratio (Figure 17). This empirical law is the first one to enable a quick consideration of kerosene vapor explosion consequences on the tank in the case of an aircraft perforation by ammunition. But this law should be adapted depending on the volume of the tank.

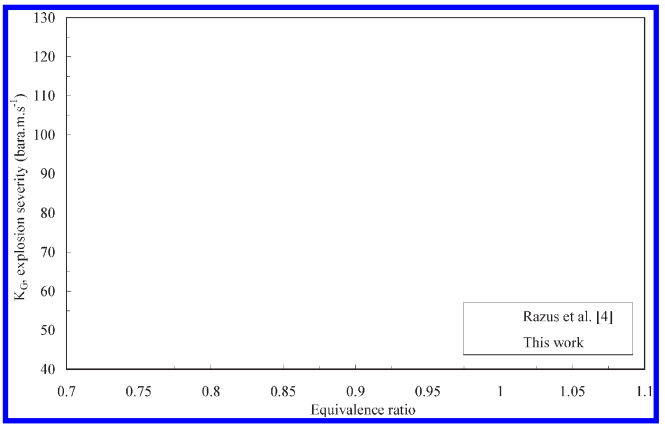

Figure 21. K_G of propylene−air mixtures at 1 bara initially compared to the present empirical laws.

$$K_{st} = \sqrt[3]{1}\left.\frac{dP}{dt}\right|_{max,\ 1m^3} = \frac{P_{expl}}{\tau_{expl}} \tag{13}$$

3.6. Estimation of the Volume Effect. The maximum time derivative of the pressure is given (eq 14) proportionally to K_G with a parabolic function of the tank volume, which corresponds to MIRAGE results (Figure 18). Each coefficient of this second-order equation depends also on the energy (eq 15). The resulting empirical law is compared on a wide range of test cases that represent all the possible range that can be met in relationship with air system (Figure 19). This illustrates the large field of validity of the empirical laws proposed in this work.

$$\left.\frac{dP}{dt}\right|_{vol} = (\alpha \mathrm{vol}^2 + \beta \mathrm{vol} + \gamma)\left.\frac{dP}{dt}\right|_{1m^3} \tag{14}$$

$$\begin{aligned} \alpha &= -2 \times 10^{-6}E^2 + 0.0041E - 1.0488 \\ \beta &= 5 \times 10^{-6}E^2 - 0.0097E + 2.5959 \\ \gamma &= -3 \times 10^{-6}E^2 + 0.0056E - 0.5473 \end{aligned} \tag{15}$$

3.7. Application to These Laws on Experimental Cases from Literature[5]. The preceding proposed laws (eqs 8 and 14) have been applied to propylene−air mixtures to be compared with experiments[5] in a 0.52 L vessel (Figure 20). The experimental ignition energy ranges from 1 to 5 mJ. These very low values are not in the range of validity of the present laws. Thus, a constant energy of 2 J is numerically used. This should help correcting the fuel nature difference. The peak pressure and the maximum rate of pressure rise are plotted for an equivalence ratio of 0.9 as a function of the initial pressure (Figure 20a) and for two different pressures as a function of the equivalence ratio (Figure 20b). Those two values are in

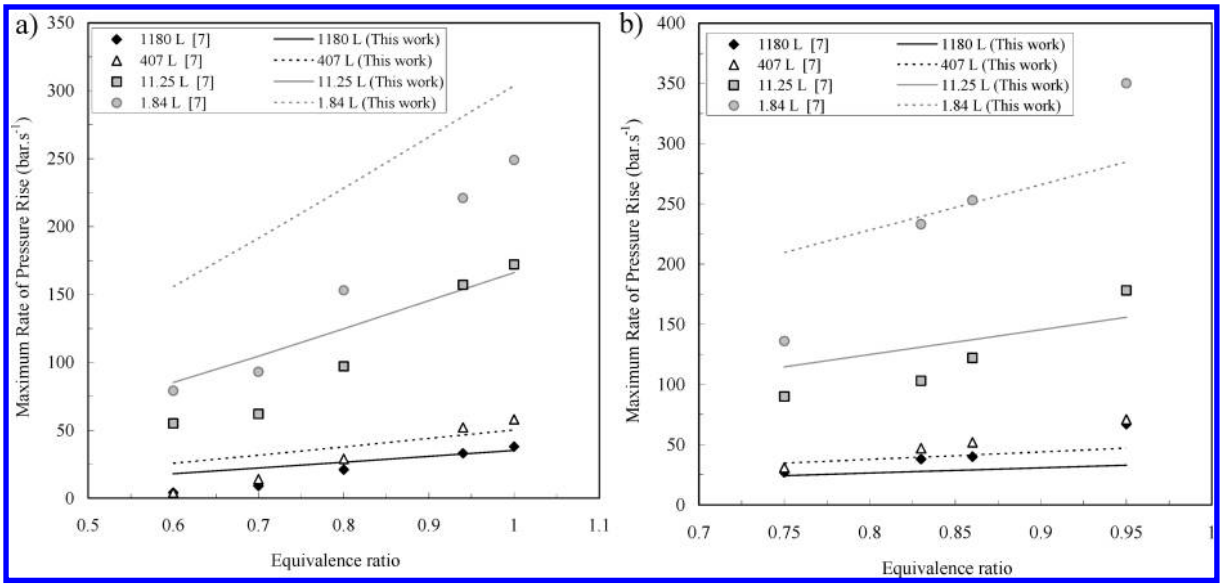

Figure 22. Maximum rate of pressure rise of methane (a) and propane (b) −air mixtures at 1 bara initially compared to the present empirical laws for four different volumes.

good agreement, and K_G (Figure 21) is also predicted with in an acceptable range.

Then, the empirical law (eq 14) has been applied to be compared with methane−air (Figure 22a) and propane−air (Figure 22b) mixtures on different volumes (1.84−1180 L) and equivalence ratio (0.6−1) at an initial pressure of 1 bara. The experimental ignition energy is mentioned to be varied from 1 mJ to 27 J depending on the vessel and on the test.[8] For MIRAGE, a constant initiation energy E of 10 mJ is numerically chosen. This explains, in addition to the differences on the hydrocarbons nature, the possible large discrepancies that are observed (Figure 22). Nevertheless, the estimation of the maximum rate of pressure rise is in the right order. On the basis of these comparisons for a wide range of equivalence ratio (0.6−1) and of initial pressure (0.5−1 bara), the agreement is judged to be satisfactory, and the discrepancies are mainly attributed to the fuel nature (probably insufficiently taken into account despite the consideration of the laminar burning speed, of the molar mass, of the isobaric heat capacity, of the combustion enthalpy, and of the computation of the equivalence ratio which naturally depends on the fuel nature through the stoichiometric relationship).

The empirical laws from the present work (from 0.4−2 m^3) appear to be adaptable to a large variety of test cases, even for a wide range of volume (here 5.2×10^{-4} to 1.18 m^3). It is visible that the proposed laws are more suitable for kerosene because they are based on corresponding vapor explosions, but due to the relatively good agreement in comparison with open literature data they could be extended to other gaseous hydrocarbons explosions in closed vessels.

4. Conclusion

The vulnerability of an air system is notably linked to kerosene explosion by ignition of ammunition impact. The violent combustion reaction occurs in gas phase because the air that is present is found in a premixed reactive mixture with gaseous fuel due to liquid fuel evaporation. This phenomenon depends on the ambient temperature and pressure, notably. Before estimating the explosion severity in real configurations with compartments and a pressure-controlled venting system, it is required to study the kerosene explosion for a single volume. By using a detailed chemical mechanism of decane (207 species, 1592 reactions), which is shown to be representative of kerosene surrogate, a parametric study is conducted by means of the numerical simulation tool MIRAGE. The code is validated on data from literature and an example is given with adapted combustion mechanism, GRIMECH. The problem of the explosion initiation has been briefly presented. The ignition energy (from 5 to 1000 J in electric spark configurations), the equivalence ratio in air (from 0.3 to 2.19), the tank pressure (from 1 to 1.8 bara), and its volume (from 0.4 to 2 m^3) are varied in the present study. The maximum pressure after explosion is found to depend linearly on the initial pressure but also not linearly on the ignition pressure and equivalence ratio. The explosion severity is found to depend on the ignition energy but also strongly on the volume. Empirical laws have been proposed to estimate the explosion characteristics depending on the configuration. The expressions of the laws have been written to be generalized as much as possible. These laws have been applied to cases from literature and the agreement is found to be acceptable. Apart from this work, a global Arrhenius law has been notably proposed with two sets of parameters depending on the temperature range to properly consider the kerosene consumption in another multiphysics simulation tool with compartments. The works will be pursued in this way to consider multicompartments configurations with a venting system.

Acknowledgment. The authors would like to give sincere thanks to P. Boureau for her help involving the English writing and to P. Dagaut for having accepted to share its source file of combustion mechanism. J. M. Pascaud is acknowledged for his collaboration on this project. The present work has been carried out with the contribution of the Délégation Générale à l'Armement and the Centre d'Etudes de Gramat.